

# Demystifying the triplet state and the quenching mechanism of self-assembled fluorenoazomethines

Derek Tsang<sup>1</sup>, Marie Bourgeaux, W.G. Skene\*

Department of Chemistry, University of Montreal, Pavillon J.A. Bombardier, C.P. 6128, succ. Centre-ville, Montreal, Que. H3C 3J7, Canada

Received 10 March 2007; received in revised form 2 May 2007; accepted 15 May 2007

Available online 18 May 2007

## Abstract

The steady-state and time-resolved photophysical investigation of fluorene derivatives revealed their fluorescence is lowered upon incorporating an azomethine linkage. The heteroconjugated bond deactivates the singlet excited state by nonradiative modes of energy dissipation including internal conversion. Similarly, the azomethine bond quenches the triplet state, but it does not increase the yield of the intrinsically formed manifold by otherwise enhancing the amount of intersystem crossing. A series of aliphatic and partially conjugated azomethines were used to probe the quenching mechanism of triplet deactivation of fluorene derivatives. Although the measured rate constants ( $2 \times 10^7$ – $1 \times 10^{10} \text{ M}^{-1} \text{ s}^{-1}$ ) for triplet quenching with various azomethines were lower than diffusion controlled processes, the endothermic energy transfer process is highly efficient when an azomethine bond is covalently bound to the triplet producing chromophore. Efficient intramolecular energy transfer is responsible for quenching the inherently formed triplet state within 10 ns leading to the absence of any detectable transients by laser flash photolysis. Steady-state photolysis at 254, 300, and 350 nm confirmed the azomethines are photostable and they do not photoisomerize.

Crown Copyright © 2007 Published by Elsevier B.V. All rights reserved.

**Keywords:** Azomethine; Triplet quenching; Laser flash photolysis; Self-quenching

## 1. Introduction

Conjugated polymers are an interesting class of compounds that have attracted much attention in the areas of materials science and organic synthesis alike. Their appeal to materials research is in part due to their electrochemical properties that are ideally suited for functional devices such as field effect transducers [1–3], solar cells [4–7], low power consumption emitting devices [8–10], and plastic electronics [11,12]. These materials also exhibit interesting photophysics that are well suited for light emitting devices and flexible light displays [13–16]. Owing to the many commercial applications [17], organic synthesis has played a major role in providing new materials with enhanced properties while overcoming the many synthetic challenges to provide these sought after materials. Fluorene based polymers have been extensively studied because of their high fluorescence yields and photophysical

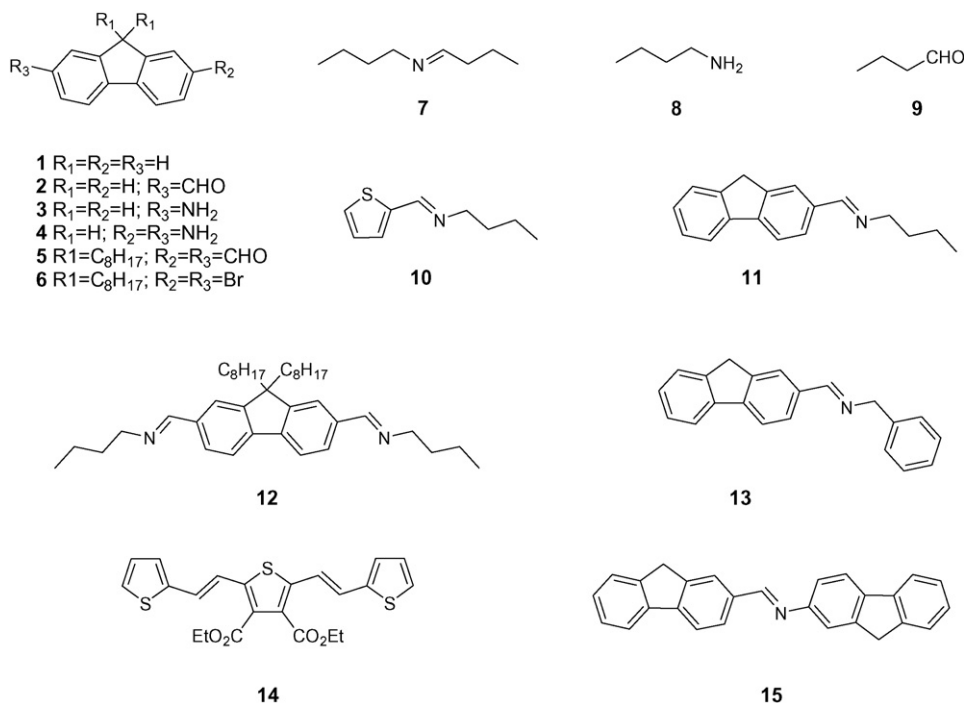
properties that are suitable for emitting devices in which they play a pivotal role as the emitting layer [16,18,19]. Although the photophysics of fluorene and its various derivatives have been widely investigated [20–23], many synthetic challenges still exist such as inconsistent reproducibility, problematical purification from residual metal catalysts, and stringent reaction conditions.

An alternate to current coupling methods for the synthesis of conjugated compounds are azomethines ( $-\text{N}=\text{C}-$ ). This is in part due to their isoelectronic properties relative to their carbon analogues [24,25], while having the advantage of easy synthesis that do not require the use of stringent reaction conditions or metal catalysts. Furthermore, azomethines can also be purified easily, unlike their carbon analogues. The recent introduction of new stable aminothiophenes [26] and the fluorene derivatives illustrated in Scheme 1 have renewed the interest in azomethines because of their promising properties that are compatible with functional materials [27–30]. Compounds derived from these amino monomers, such as **14** and **15**, possess properties [31–34] that successfully address the serious problems limiting the use of previous investigated homoaryl azomethines as materials in functional devices. Even though fluorene (**1**) exhibits

\* Corresponding author. Tel.: +1 514 340 5174; fax: +1 514 340 5290.

E-mail address: [w.skene@umontreal.ca](mailto:w.skene@umontreal.ca) (W.G. Skene).

<sup>1</sup> Current address: University of Toronto, Toronto, Canada.



Scheme 1. Compounds examined and some representation analogues.

a high fluorescence quantum yields, it undergoes intersystem crossing (ISC) to populate its triplet state. This manifold shift is problematic for emitting devices because it results in unwanted delayed emission and phosphorescence that is bathochromically shifted from the desired emission. Interestingly, no triplet state was visible by laser flash photolysis (LFP) for any of the fluorenoazomethines while one is detectable for its amino and aldehyde precursors [35]. Similarly, thiopheno azomethines (**14**) also exhibited the absence of a triplet signal [31,32,34]. Therefore, incorporating an azomethine bond has an important influence on the photophysics of these materials. Despite their prolific use and well studied behavior for protecting functional groups in organic synthesis, the photophysics of azomethines and the means by which they affect the excited states of chromophores have not been thoroughly examined. While only a few studies have examined fluorene azomethines [29,36–38], none have extensively examined the photophysics and the deactivation modes of these novel conjugated compounds. Information regarding the excited state including the triplet manifold of azomethines and knowledge of their quenching mechanism are pivotal for determining their suitability as advanced materials for functional devices.

Our long-standing interest in conjugated azomethines [26,31–34,39] prompted us to investigate the effect of azomethine quenchers upon the photophysics of fluorene derivatives as a means to better understand the main phenomena involved in the mechanism of excited state deactivation. In particular, we have examined the triplet state of these materials by time-resolved means in order to determine the influence of various azomethines on the fluorene triplet state. The rate constants of triplet quenching were measured in hope of providing information regarding the intramolecular self-quenching of conjugated azomethines.

The photostability of the simple fluorenoazomethines was also investigated.

## 2. Experimental

### 2.1. Materials

All reagents were commercially available from Aldrich and were used as received unless otherwise stated. Anhydrous and deaerated solvents were obtained via a Glass Contour solvent purification system. Isopropanol was dried over activated molecular sieves and stored under nitrogen.  $^1H$  NMR spectra were recorded on a Bruker 400 spectrometer with the appropriate deuterated solvents. Compound **5** was prepared from the commercially available **6** according to known methods [35]. Compounds **14** and **15** were prepared in the same manner as previous examples [34,35].

### 2.2. Spectroscopic measurements

Absorption measurements were done on a Cary-500 spectrometer and fluorescence studies were carried out on an Edinburgh Instruments FLS-920 fluorimeter after deaerating the samples thoroughly with nitrogen for 20 min. The fastest lifetime resolution for the fluorescence kinetics is 900 ps. Fluorescence quantum yields were measured at  $10^{-5}$  M by exciting the corresponding compounds at an optically matched wavelength in anhydrous spectroscopic grade acetonitrile and compared to fluorene ( $\phi = 0.8$ ) excited at the same wavelength [35,40–42]. The actinometer absorbencies, and those of the compounds, were matched at the excitation wavelength to within 5%.

### 2.3. Laser flash photolysis (LFP)

The triplet–triplet absorption spectra were measured in anhydrous and deaerated acetonitrile using a mini-LFP system from Luzchem Research Inc., of Ottawa excited either at 266 nm from the forth harmonic or at 355 nm from the third harmonic of a Continuum YAG:Nd Sure-lite laser. The laser power levels were adjusted such that 60 and 100 mJ of energy resulted per shot at 266 and 355 nm, respectively. Samples were prepared with an absorbance between 0.25 and 0.35 dissolved in anhydrous acetonitrile in static quartz cuvettes. A flow cell was used where indicated. All samples were purged with nitrogen for at least 20 min before undertaking LFP analyses.

### 2.4. Stern–Volmer quenching studies

The triplet states of various fluorenes were quenched using different azomethines, an amine, and an aldehyde. A fluorene sample was prepared in anhydrous acetonitrile with an absorbance between 0.25 and 0.35 at the laser excitation wavelength and it was then deaerated with nitrogen for a minimum of 20 min. A stock solution of quencher was prepared in anhydrous acetonitrile at a mM concentration and then it was deaerated. Known volumes of the quencher were added to the cuvette containing the fluorene via a syringe and the resulting first order triplet decays were recorded at the  $\lambda_{\text{max}}$  for the corresponding fluorene. The quencher **7** was kept on ice until it was used for the quenching experiments in order to prevent its premature decomposition products.

### 2.5. Steady-state irradiation

All irradiation studies were done in purged, anhydrous acetonitrile and oxygen saturated solutions held in quartz cuvettes. The solution concentration was adjusted to give an absorbance of 1 at the irradiation wavelength. All experiments were done with 14 lamps in a Luzchem photoreactor at full illumination. The samples were periodically removed and the  $^1\text{H}$  NMR and absorption spectra were recorded in order to confirm the absence of decomposition.

### 2.6. Synthetic procedures

#### 2.6.1. Butyl-butylidene-amine (**7**)

Butylamine (1 mL, 10.1 mmol) was added dropwise to butyraldehyde (1 mL, 11.1 mmol) with stirring. The water formed from the exothermic reaction was physically removed by a Pasteur pipette, and the clear, colourless oil was further dried with 4 Å molecular sieves. Excess butylamine and butyraldehyde were removed *in vacuo*. All samples of aliphatic imine were kept under nitrogen and on ice until used in order to prevent decomposition.

#### 2.6.2. *N*-((Thiophen-2-yl)methylene)butan-1-amine (**10**)

Thiophene-2-carboxaldehyde (1 mL, 10.7 mmol) was mixed with anhydrous dichloromethane (4 mL). Anhydrous  $\text{MgSO}_4$

was added, followed by *n*-butylamine (2 mL, 20.2 mmol). The system was kept under nitrogen and stirred for 4 h. The resulting salts were filtered off and the filtrate was evaporated *in vacuo* to yield the desired product as a yellow liquid. The compound was used immediately for quenching studies owing to its rapid decomposition, which limited its characterization by standard methods. This notwithstanding, accurate kinetic measurements with **10** were possible by keeping the compound on ice until used. Little decomposition was observed under the diluted quenching measurements.

#### 2.6.3. *N*-((9*H*-Fluoren-7-yl)methylene)butan-1-amine (**11**)

Fluorene-2-carboxaldehyde (56 mg, 0.29 mmol) was dissolved in isopropanol (25 mL), to which *n*-butylamine (1 mL, 10.1 mmol) was added along with a catalytic amount of trifluoroacetic acid. The system was kept under nitrogen and it was refluxed overnight. The solvent and the excess amine were removed *in vacuo* to afford the pure title compound as pale-yellow crystals (58 mg, 81%).  $^1\text{H}$  NMR (400 MHz,  $\text{CDCl}_3$ ):  $\delta$  = 8.36 (s, 1H), 8.00 (s, 1H), 7.83 (d, 2H), 7.71 (d, 1H), 7.58 (d, 1H), 7.41 (t, 1H), 7.37 (dt, 1H), 3.96 (s, 2H), 3.67 (t, 2H), 1.75 (m, 2H), 1.47 (m, 2H), 0.99 (t, 3H).  $^{13}\text{C}$  NMR (400 MHz,  $\text{CDCl}_3$ ):  $\delta$  = 161, 144.5, 144.4, 144.0, 141.5, 135.0, 128.0, 127.7, 127.3, 125.6, 124.4, 120.8, 120.2, 62.0, 37.0, 34.0, 21.0, 14.0. MS:  $m/z$  250.15903 [ $M + \text{H}$ ] $^+$ .

#### 2.6.4. (30*E*)-*N*-((2-((*E*)-(Butylimino)methyl)-9,9-dioctyl-9*H*-fluoren-7-yl)methylene)butan-1-amine (**12**)

9,9'-Dioctyl-fluorene-2,7-dicarboxaldehyde (73 mg, 0.16 mmol) was dissolved in isopropanol (10 mL) under nitrogen. One drop of catalytic trifluoroacetic acid was added, followed by the dropwise addition of *n*-butylamine (1 mL, 10.1 mmol) over a period of 10 min while stirring. The solution was then refluxed for 4 h and the excess volatile reagents were removed under *vacuo*. A yellow oil was recovered, which crystallized into yellow-orange crystals overnight to yield the title compound (74.7 mg, 82%).  $^1\text{H}$  NMR (400 MHz, acetone- $d_6$ ):  $\delta$  = 8.42 (s, 1H), 7.90 (m, 2H), 7.79 (dd, 1H), 3.63 (t, 2H), 2.11 (m, 2H), 1.68 (m, 2H), 1.44 (m, 2H), 1.21 (m), 1.17 (m), 0.99 (t, 3H), 0.95 (t, 3H), 0.62 (m, 2H).  $^{13}\text{C}$  NMR (400 MHz,  $\text{CDCl}_3$ ):  $\delta$  = 161.1, 152.4, 143.0, 136.4, 128.3, 123.3, 121.1, 61.3, 55.2, 40.4. MS:  $m/z$  557.47925 [ $M + \text{H}$ ] $^+$ .

#### 2.6.5. *N*-((9*H*-Fluoren-7-yl)methylene)(phenyl)-methanamine (**13**)

Fluorene-2-carboxyaldehyde (67.3 mg, 0.35 mmol) was dissolved in anhydrous dichloromethane (2 mL). Benzylamine (0.31 mL, 2.84 mmol) was added dropwise to the aldehyde solution while stirring, followed by a small amount of anhydrous  $\text{MgSO}_4$ . The solution was stirred for 4 h at room temperature, filtered, and then evaporated *in vacuo* to yield the title compound (71 mg, 72%) as a solid.  $^1\text{H}$  NMR (400 MHz, acetone- $d_6$ ):  $\delta$  = 8.59 (s, 1H), 8.08 (s, 1H), 7.95 (t, 2H), 7.86 (d, 1H), 7.62 (d, 1H), 7.36–7.42 (m, 7H), 4.84 (s, 2H), 4.00 (s, 2H).

### 3. Results and discussion

#### 3.1. Azomethine synthesis

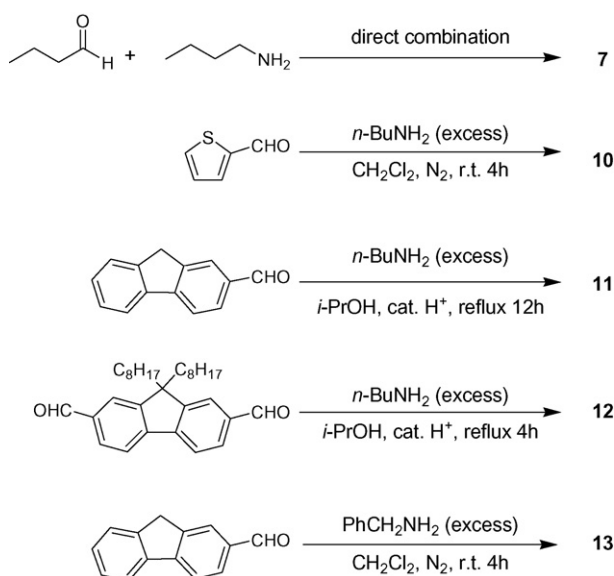
Despite our previous success in synthesizing conjugated azomethines via simple means [31–35,39,43], the azomethine derivatives (**7**, **10–13**) reported in Scheme 1 were problematic. The azomethine bond is robust and it resists hydrolysis when a highly conjugated compound is formed. However, it is highly susceptible to acid catalyzed hydrolysis when the bond formed is only moderately conjugated as with **10–13**. Successful synthesis of the azomethine for their use as quenchers was possible by using an excess of the butylamine in order to displace the equilibrium in favor of the products of the otherwise highly reversible reaction, according to Scheme 2. The amine was often used in a 10–20-fold excess, which considerably shortened the reaction times. The aryl azomethine derivatives were highly stable once formed providing they were kept under an inert atmosphere. The synthesis of **7** was exceptionally difficult owing to its high propensity to decompose. Although a previous protocol for the synthesis of this compound exists [44], the desired product could not be isolated in high purity for its subsequent use in quenching studies. The compound rapidly decomposed when exposed to common chromatographic purifications. However, using the reagents as solvent yielded exclusively the desired product that could easily be isolated in high purity by evaporating the unreacted reagents. Compound **7** was sufficiently stable under an inert atmosphere permitting its use for time-resolved quenching studies.

#### 3.2. Fluorescence measurements

Previous studies of **14** showed it exhibited fluorescence two orders of magnitude smaller than its oligothiophene analogue [31,34]. The low fluorescence quantum is not surprising

since thiophenes efficiently deactivate their singlet excited state by ISC to populate their triplet state. However, the triplet of **14** was not detected in high amounts by laser flash photolysis (LFP), while a triplet at 77 K was visible. Deactivation of the singlet excited state by internal conversion (IC) was confirmed by fluorescence measurements at 77 K, at which temperature the quantum yields of IC can be obtained according to:  $\Phi_{\text{fl}}(77\text{ K}) - \Phi_{\text{fl}}(\text{RT}) \approx \Phi_{\text{IC}}$ . The triplet state is formed in less than 10% according to the energy conversation equation:  $\Phi_{\text{fl}} + \Phi_{\text{ISC}} + \Phi_{\text{IC}} \approx 1$ . Similarly, **15** also did not show any signal by LFP as seen in Fig. 1. Even though fluorenes are highly fluorescent ( $\Phi_{\text{fl}}(\text{1}) = 0.72$ ) [35,45] the remaining 30% in energy loss occurs by ISC leading to a visible triplet by LFP. A strong signal comparable to xanthone was therefore expected under identical experimental conditions. The absence of a detectable triplet by LFP for **15**, shown in Fig. 1, is therefore surprising. Time-resolved fluorescence measurements were subsequently done to provide insight into the azomethine quenching effect on the singlet excited state.

The radiative ( $k_r$ ) and nonradiative ( $k_{\text{nr}}$ ) rate constants reported in Table 1 are considerably different for **14** and **15** providing a preliminary means by which to assess the influence of the azomethine upon the singlet excited state. The large  $k_r$  implies a high fluorescence yield since the value is calculated from the fluorescence quantum yield and the fluorescence lifetime according to  $k_r = \Phi_{\text{fl}}/\tau$ . The observed low value for **14** implies the singlet state is deactivated by nonradiative channels. The low  $k_{\text{nr}}$  for **14** relative to **15** further suggests the singlet state dissipates its energy by means of IC rather than ISC. This is corroborated by the low temperature fluorescence measurements seen in the inset of Fig. 1 showing little fluoresce increase at 77 K relative to room temperature. Significant increase in the emission at 77 K would occur if IC was a preferred mode of energy dissipation. The fluorescence quantum yields and the singlet excited state lifetimes of compounds **10–13** were examined to determine the effect of the simple unconjugated azomethine linkage



Scheme 2. Reaction scheme for the synthesis of various azomethines from Scheme 1.

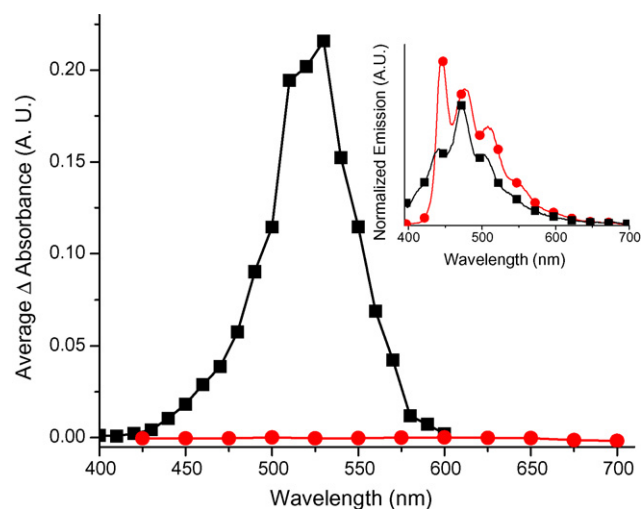


Fig. 1. Transient absorption spectra of **15** (●) and xanthone (■) excited at 266 nm in anhydrous acetonitrile. Inset: fluorescence of **15** measured at room temperature (■) and 77 K (●).

Table 1

Quantum yields and other singlet excited state properties of various chromophores

Compound	$\lambda_{\text{abs}}$ (nm) <sup>a</sup>	$\lambda_{\text{em}}$ (nm) <sup>b</sup>	$\Phi_{\text{fl}}$ <sup>c</sup>	$\tau$ (ns) <sup>d</sup>	$k_{\text{r}}$ ( $\times 10^7 \text{ s}^{-1}$ ) <sup>e</sup>	$k_{\text{nr}}$ ( $\times 10^8 \text{ s}^{-1}$ ) <sup>f</sup>
<b>1</b>	261	302	0.72	10	7.0	0.3
<b>2</b>	316	365	0.82	1.2	68.3	1.5
<b>5</b>	326	383	0.72	1.2	59.5	2.4
<b>10</b>	253	274	0.02	4.7	0.4	2.1
<b>11</b>	305	330	0.10	2.3	4.4	3.9
<b>12</b>	306	387	0.60	0.9	66.7	4.4
<b>13</b>	307	389	0.25	6.7	3.7	1.1
<b>14</b> <sup>g</sup>	440	534	0.003	13.2	0.02	0.8
<b>15</b> <sup>h</sup>	361	445	0.40	1.1	36.4	5.5

<sup>a</sup> Absorption maximum.

<sup>b</sup> Fluorescence maximum.

<sup>c</sup> Fluorescence quantum yield relative to fluorene [50,54].

<sup>d</sup> Fluorescence lifetime.

<sup>e</sup> Radiative rate constant  $k_{\text{r}} = \Phi_{\text{fl}}/\tau_{\text{fl}}$ .

<sup>f</sup> Nonradiative rate constant  $k_{\text{nr}} = k_{\text{r}}(1 - \Phi_{\text{fl}})/\Phi_{\text{fl}}$ .

<sup>g</sup> From Bourgeaux et al. [31,32].

<sup>h</sup> From Pérez Guarín et al. [35].

on the singlet excited manifold. The calculated rate constants in Table 1 for **10–13** for both the radiative and nonradiative decays are similar to **15**. This suggests the simple aliphatic azomethine linkage does not promote ISC to artificially populate the triplet manifold, rather it affects the singlet excited state by providing additional modes of energy dissipation resulting in efficient IC. The decrease in fluorescence yields for the azomethine fluorene derivatives relative to its aldehyde precursor (**2** versus **11** and **5** versus **12**) provide further evidence that the simple azomethine nonradiatively deactivates the singlet excited state. Similar to **14** and **15**, no triplet was detected by LFP for any of the aliphatic azomethine derivatives in Table 1. The combined time-resolved and steady-state fluorescence measurements concomitant with the qualitative absence of LFP signal provide indirect proof that the azomethine does not increase the amount of inherently formed triplet by ISC, rather it quenches the formed triplet state by intramolecular energy transfer. The azomethine accordingly deactivates the singlet excited state by providing nonradiative channels for energy dissipation.

### 3.3. Quenching measurements

The capacity of azomethines to quench the triplet state was examined with triplet producing fluorenes in the presence of various azomethines. Since compounds **10–13** did not produce any detectable signal by LFP, the triplet states of **1–6** were examined. Not only do these compounds provide information regarding the effect of electronic groups on the transient absorption spectrum, they are also the precursors used in the synthesis of conjugated fluorenes such as **15**. Furthermore, a detectable triplet for fluorenes **2–6** would prove their triplets are indeed inherently formed. The added advantage of these precursors is they would also confirm if an azomethine linkage appended to the triplet producing chromophores is responsible for quenching the triplet. The triplet–triplet absorption spectra observed for **1–6** are tabulated in Table 2 and a representative transient absorption

Table 2

Laser flash photolysis of substituted fluorenes exhibiting triplet states upon excitation at 266 nm in anhydrous acetonitrile

Compound	$\lambda_{\text{max}}$ (nm) <sup>a</sup>	$\tau$ ( $\mu\text{s}$ ) <sup>b</sup>	$k$ ( $\times 10^5 \text{ s}^{-1}$ ) <sup>c</sup>	$k_{\text{q}}$ ( $\times 10^7 \text{ M}^{-1} \text{ s}^{-1}$ ) <sup>d</sup>		
				7	8	9
<b>1</b>	375	0.6	16.5	250	0.3	1
<b>2</b>	440	6.3	1.6	30		
<b>3</b>	450	8.1	1.2	2		
<b>4</b>	437	2.4	4.1	2	1	0.3
<b>5</b>	470	5.9	1.4	5	0.01	0.4
<b>6</b>	405	2.2	4.6	16		

The triplet quenching ( $k_{\text{q}}$ ) was measured with the addition of **7**, **8**, or **9**.

<sup>a</sup> Triplet–triplet absorption maximum.

<sup>b</sup> Triplet lifetime measured at triplet–triplet absorption maximum.

<sup>c</sup> Rate constant of triplet decay in the absence of quencher.

<sup>d</sup> Quenching rate constant in the presence of quencher.

spectrum for the fluorenes is found in Fig. 2. Despite a negative signal resulting from strong ground state bleaching, this does not interfere with the triplet absorption, which is bathochromically shifted relative to the ground state bleaching. In all cases, a strong signal with a good s/n ratio was observed as seen in the inset of Fig. 2. The observed signals were assigned to the triplet because of their characteristic unimolecular decays occurring on the  $\mu\text{s}$  time scale. Furthermore, the signals were quenched with standard triplet quenchers including oxygen, 1,3-cyclohexadiene, 1-methylnaphthalene, and  $\beta$ -carotene. It is evident according to Table 2 that all the studied compounds exhibited a triplet visible in the range of 375 and 470 nm, while the maximum triplet–triplet absorption depends on the number and the type of the electronic groups substituted on the fluorene.

The aliphatic azomethine **7** was used as a model compound to assess the azomethine linkage's capacity to quench triplets. This simple quencher probe is also transparent at the excitation wavelengths used for the LFP measurements. This allows the addition of large amounts of the quencher if required without the risk of directly exciting it, which would otherwise lead to complicated quenching kinetics. The efficiency of **7** to deactivate a triplet was

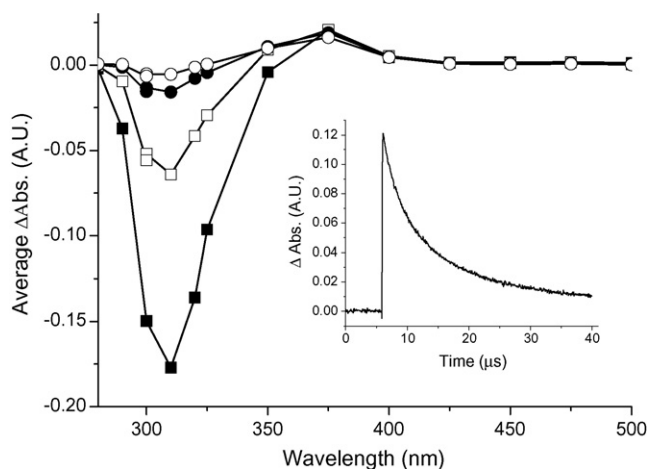


Fig. 2. Transient absorption spectrum of **1** measured in anhydrous acetonitrile at 0.6 (■), 1.1 (□), 2.2 (●), and 3.3  $\mu\text{s}$  (○) after laser irradiation at 266 nm. Inset: triplet decay of **1** monitored at 375 nm after laser pulse at 266 nm.



determined by monitoring the change in triplet decays of the fluorene derivatives in the presence of varying concentrations of the azomethine. These measurements were done at the corresponding triplet–triplet maximum absorption according to Table 2 in order to provide a good s/n ratio. First order decays were observed for the triplets of **1–6** with the addition of **7** as shown in the inset of Fig. 3. Triplet deactivation by energy transfer from the fluorene triplet to the azomethine, and hence the deactivation efficiency, corresponds to the quenching rate constant,  $k_q$ . This can be determined from the slope of the observed first order rate constant ( $k_{\text{obs}}$ ) as a function of the quencher concentration ( $[Q]$ ) according to the following Stern–Volmer equation:  $k_{\text{obs}} = k_0 + k_q[Q]$ , where  $k_0$  is the rate constant for triplet decay in the absence of quencher. Fig. 3 illustrates the capacity of **7** to deactivate the triplet of the fluorene derivatives with varying efficiencies. The calculated  $k_q$  values reported in Table 2 range from 0.2 to  $25 \times 10^8 \text{ M}^{-1} \text{ s}^{-1}$ . These rate constants are slower than diffusion controlled ( $10^{10} \text{ M}^{-1} \text{ s}^{-1}$ ) processes in acetonitrile [46]. This implies the energy transfer quenching process from the fluorene to **7** is endothermic suggesting the fluorene triplet is lower in energy than the azomethine triplet. A large quantity of azomethine is therefore required to deactivate the fluorene triplet. Nonetheless, quenching of the triplet by the azomethine does occur.

Quenching of the various fluorene triplets was additionally done with butylamine (**8**) and butyraldehyde (**9**) in order to validate the efficiency of triplet quenching measured for **7**. The systematically slower quenching rate constants for **8** and **9** relative to **7**, confirm the aliphatic azomethine is an efficient triplet quencher. According to the inset of Fig. 3, the addition of **7** accelerates the triplet decay, but it does not decrease the signal intensity. This is indicative of dynamic quenching whereby the azomethine must diffuse to the excited chromophore and deactivate the excited state within the triplet's lifetime [47–49]. The quenching rate constant and hence the efficiency of triplet deactivation is dependent upon the azomethine concentration.

The conjugated azomethines **10** and **11** were also examined for their triplet quenching capacity. Since the azomethine is con-

Table 3

Quenching of xanthone triplet with various azomethines produced upon excitation at 355 nm in anhydrous acetonitrile

Quencher	$k_q (\times 10^9 \text{ M}^{-1} \text{ s}^{-1})$
1-Methylnaphthalene	7.0
<b>10</b>	9.0
<b>11</b>	10

nected directly to an aryl unit for these two quenchers, they are more conjugated than **7**. Therefore, they are expected to have lower triplet energies resulting in faster quenching rate constants and more efficient triplet deactivation. Xanthone was selected as the triplet source instead of the fluorenes because it can be selectively irradiated at 355 nm while **10** and **11** are spectroscopically transparent at this wavelength. This avoids problems occurring with direct excitation of the quenchers that would otherwise lead to complicated decay kinetics and to multiple transients. The measured rate constants in Table 3 are 10 times faster than for **7**. The greater degree of conjugation of **10** and **11** results in a lower triplet energy than **7**, leading to exothermic quenching of the xanthone triplet by energy transfer. This is confirmed by the measured  $k_q$  value ( $7 \times 10^9 \text{ M}^{-1} \text{ s}^{-1}$ ) for the quenching of xanthone by 1-methylnaphthalene, which is a known efficient quencher because of its low lying triplet that is capable of exothermically quenching most triplets [50]. The faster  $k_q$  for **10** and **11** relative to **7** confirms the conjugated azomethines more efficiently quench the triplet compared to their aliphatic analogues.

The observed rate constants for **7**, **10**, and **11** provide evidence that the azomethine quenches the fluorene triplet state. Although the measured rate constants are not diffusion controlled, implying inefficient triplet quenching, the fast rate constants nonetheless confirm triplet quenching is possible. The complete suppression of any visible triplet by LFP with the azomethine-chromophore adducts is a result of the large effective azomethine concentration resulting in efficient triplet quenching by intramolecular energy transfer. The effective quenching concentration for intramolecular quenching processes is 1 M while the average triplet concentration produced upon laser excitation is ca.  $\mu\text{M}$ . The  $10^6$  concentration difference is responsible for efficient deactivation of the fluorene triplet. This is empirically validated by substituting the intramolecular quencher concentration into the standard Stern–Volmer rate equation above along with  $k_q$  for **7**, leading to a triplet lifetime of 10 ns. Given the fastest lifetime that can be resolved by the LFP system is  $\sim 100$  ns, the azomethine must rapidly quench the triplet such that it cannot be detected within the time resolution of the LFP system.

Since undesired transients that contaminate pristine emission occur from the triplet manifold, ideal fluorenes to be used as the emitting layer in functional devices must therefore possess high fluorescence quantum yields with little ISC. Or, if the triplet is inherently formed, its deactivation must occur by nonemissive means. Electrochemically induced excitation selection rules for functioning devices further complicates matters such that each exciton produces 75% triplets and only 25% singlets. This

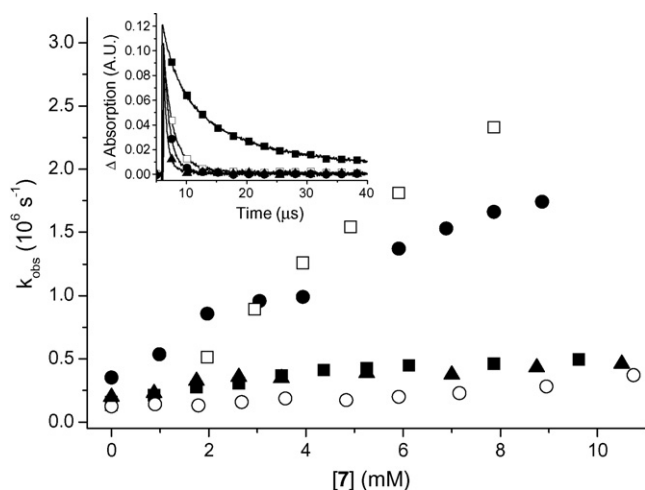


Fig. 3. Triplet quenching of various fluorenes as a function of **7** added: **2** (□), **3** (○), **4** (▲), **5** (■), and **6** (●). Inset: triplet decay of **2** measured at 440 nm with 0 mM (■), 2.9 mM (□), 4.9 mM (●), and 7.9 mM (◆) of **7**.

manifold shift highly populates the triplet level and potentially promotes undesired phosphorescence that is bathochromically shifted relative to the fluorescence. Long-lived species additionally result from this process, which contaminate the desired pristine fluorescence. Fluorene azomethines are therefore suitable candidates for emitting devices since the unwanted triplet state is efficiently deactivated by nonradiative means affording pristine emission originating from only the singlet state.

### 3.4. Photostability

Like their carbon analogues, azomethines also possess two geometric isomers (*E* and *Z*) as shown in Fig. 4. Photoisomerization resulting in the interconversion of the two isomers is possible as found with azobenenes and stilbenes [51–53]. Even though the time-resolved transient studies confirmed that the azomethines nonradiatively deactivate their triplet states, steady-state irradiation was used to investigate a possible deactivation by photoisomerization. Irradiation of **11** was done at 254, 300, 350 nm for various times in acetone and in dichloromethane with a total of 14 lamps in the photoreactor. These conditions are normally sufficient to induce detectable photoisomerization products with other compounds. Interconversion between the two isomers would result in spectroscopically detectable changes in both absorption and  $^1\text{H}$  NMR owing to the different degrees of conjugation of the two isomers. No change in the absorption wavelength or in the intensity was detected upon irradiating a sample at the various wavelengths for 5–15 min. The  $^1\text{H}$  NMR spectra was also unchanged after irradiating **11** for 15 min. A detectable shift in the imine proton at 8.35 ppm would occur if isomerization between the *E* and *Z* isomers was present. Moreover, the single imine peak confirms the presence of only one isomer while the unchanged integration confirms the product does not photodecompose.

Additional photodecomposition studies were undertaken with **11** and **12**. **12** exhibited extreme photostability with no detectable decomposition even after 15 h of irradiation at 300 nm according to Fig. 5. The absence of any significant decomposition under the intense photon flux confirms the robustness and the photostability of the azomethine bond. Similarly, **11** exhibited high photostability with no apparent decomposition after 3 h of intense irradiation at 254 and 300 nm. Less than 20% decomposition occurred only after 15 h of irradiation at 300 nm while the same amount of decomposition was observed after 3 h of irradiation at the more intense 254 nm wavelength. Since no photodecomposition or photoisomerization was observed for the aryl azomethines, deactivation of their excited state produced by energy transfer from a triplet donor most likely occurs by

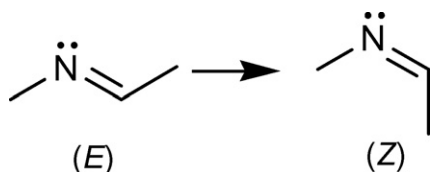


Fig. 4. The two possible geometric isomers of azomethines.

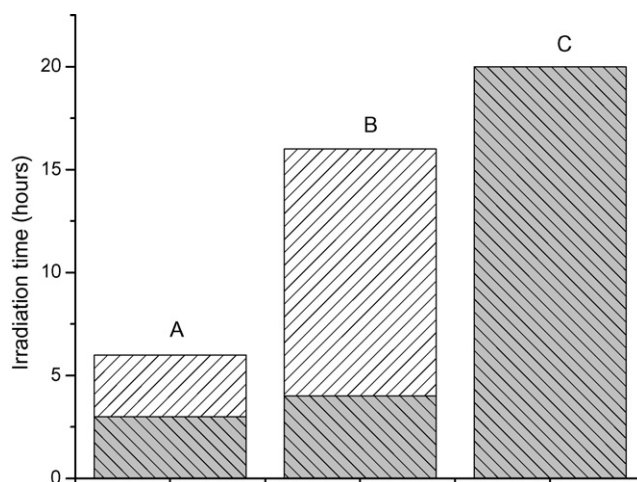


Fig. 5. Effect of irradiation time on the photostability of **11** and **12**: no decomposition (▨) and less than 20% decomposition (▩). (A) **11** irradiated at 254 nm. (B) **11** irradiated at 300 nm. (C) **12** irradiated at 300 nm.

nonradiative means and is in agreement with the fluorescence studies.

### 4. Conclusion

Steady-state and time-resolved investigations of fluorene derivatives revealed their fluorescence is significantly reduced upon incorporating an azomethine linkage, which is responsible for deactivating the singlet excited state by nonradiative modes. The heteroconjugated bond does not promote ISC to the triplet manifold; rather the azomethines efficiently deactivate the inherently formed triplet state by energy transfer. Triplet self-quenching by the conjugated azomethines via intramolecular energy transfer completely suppresses undesired long-lived emission while providing pristine fluorescence. This behavior makes the photostable fluorenoazomethines ideal replacements for currently used emission layers in functional devices owing to their intrinsic quenching properties. These suppress the unwanted triplet state that is otherwise inherently formed in high yields because of electrochemically derived selection rules leading to contaminated emission in functioning devices.

### Acknowledgements

The authors acknowledge financial support from the Natural Sciences and Engineering Research Council Canada, the Centre for Self-Assembled Chemical Structures, and additional equipment funding from the Canada Foundation for Innovation. DT thanks NSERC for an UGA scholarship and the Reactive Intermediate Student Exchange Program.

### References

- [1] A. Kraft, Chem. Phys. Chem. 2 (2001) 163–165.
- [2] G. Horowitz, Adv. Mater. 10 (1998) 365–377.
- [3] H. Thiem, P. Strohhriegel, S. Setayesh, D. d. Leeuw, Synth. Met. 156 (2006) 582–589.
- [4] M. Gratzel, J.-E. Moser, Electr. Transf. Chem. (2001) 589–644.

- [5] H. Spanggaard, F.C. Krebs, *Sol. Energy Mater. Sol. Cells* 83 (2004) 125–146.
- [6] K. Colladet, S. Fourier, T.J. Cleij, L. Lutsen, J. Gelan, D. Vanderzande, L.H. Nguyen, H. Neugebauer, S. Sariciftci, A. Aguirre, G. Janssen, E. Goovaerts, *Macromolecules* 40 (2007) 65–72.
- [7] J. Roncali, *Chem. Soc. Rev.* 34 (2005) 483–495.
- [8] M.A. Loi, C. Rost-Bietsch, M. Murgia, S. Karg, W. Riess, M. Muccini, *Adv. Funct. Mater.* 16 (2006) 41–47.
- [9] D.-H. Hwang, M.-J. Park, C. Lee, *Synth. Met.* 152 (2005) 205–208.
- [10] D. Dini, *Chem. Mater.* 17 (2005) 1933–1945.
- [11] L. Rupprecht, *Conductive Polymers and Plastics in Industrial Applications*, Society of Plastics Engineers/Plastics Design Library, Brookfield, Conn., 1999.
- [12] J.A. Rogers, Z. Bao, K. Baldwin, A. Dodabalapur, B. Crone, V.R. Raju, V. Kuck, H. Katz, K. Amundson, J. Ewing, P. Drzaic, *Proc. Natl. Acad. Sci. U.S.A.* 98 (2001) 4835–4840.
- [13] A.G. MacDiarmid, *Angew. Chem. Int. Ed.* 40 (2001) 2581–2590.
- [14] C.D. Dimitrakopoulos, P.R.L. Malenfant, *Adv. Mater.* 14 (2002) 99–117.
- [15] G. Hughes, M.R. Bryce, *J. Mater. Chem.* 15 (2005) 94–107.
- [16] P. Chen, G. Yang, T. Liu, T. Li, M. Wang, W. Huang, *Polym. Int.* 55 (2006) 473–490.
- [17] I.F. Perepichka, D.F. Perepichka, H. Meng, F. Wudl, *Adv. Mater.* 17 (2005) 2281–2305.
- [18] M. Leclerc, *J. Polym. Sci. Part A: Polym. Chem.* 17 (2001) 2867–2873.
- [19] F.B. Dias, S. Pollock, G. Hedley, L.O. Palsson, A. Monkman, I.I. Perepichka, I.F. Perepichka, M. Tavasli, M.R. Bryce, *J. Phys. Chem. B* 110 (2006) 19329–19339.
- [20] D.J.V.C. v. Steenis, O.R.P. David, G.P.F. v. Strijdonck, J.H. v. Maarseveen, J.N.H. Reek, *Chem. Commun.* (2005) 4333–4335.
- [21] U. Scherf, E.J.W. List, *Adv. Mater.* 14 (2002) 477–487.
- [22] J. Jo, C. Chi, S. Hoeger, G. Wegner, D.Y. Yoon, *Chem. Eur. J.* 10 (2004) 2681–2688.
- [23] Y. Geng, A. Trajkovska, D. Katsis, J.J. Ou, S.W. Culligan, S.H. Chen, *J. Am. Chem. Soc.* 124 (2002) 8337–8347.
- [24] C. Wang, S. Shieh, E. LeGoff, M.G. Kanatzidis, *Macromolecules* 29 (1996) 3147–3156.
- [25] C.-J. Yang, S.A. Jenekhe, *Chem. Mater.* 3 (1991) 878–887.
- [26] M. Bourgeaux, S. Vomsheid, W.G. Skene, *Acta Cryst. E62* (2006) o5529–o5531.
- [27] W.G. Skene, *WO* 2,005,073,265 (2005).
- [28] O. Thomas, O. Inganäs, M.R. Andersson, *Macromolecules* 31 (1998) 2676–2678.
- [29] F.-C. Tsai, C.-C. Chang, C.-L. Liu, W.-C. Chen, S.A. Jenekhe, *Macromolecules* 38 (2005) 1958–1966.
- [30] N. Kiriy, V. Bocharova, A. Kiriy, M. Stamm, F.C. Krebs, H.-J. Adler, *Chem. Mater.* 16 (2004) 4765–4771.
- [31] M. Bourgeaux, S.A. Perez Guarin, W.G. Skene, *J. Mater. Chem.* 17 (2007) 972–979.
- [32] S. Dufresne, M. Bourgeaux, W.G. Skene, *J. Mater. Chem.* 17 (2007) 1166–1177.
- [33] M. Bourgeaux, W.G. Skene, *Macromolecules* 40 (2007) 1792–1795.
- [34] S.A. Pérez Guarin, M. Bourgeaux, S. Dufresne, W.G. Skene, *J. Org. Chem.* 72 (2007) 2631–2643.
- [35] S.A. Pérez Guarin, S. Dufresne, D. Tsang, A. Sylla, W.G. Skene, *J. Mater. Chem.* 17 (2007) 2801–2811.
- [36] S.-H. Jung, T.-W. Lee, Y.C. Kim, D.H. Suh, H.N. Cho, *Opt. Mater.* 21 (2003) 169–173.
- [37] N. Giuseppone, J.-M. Lehn, *Chem. Eur. J.* 12 (2006) 1723–1735.
- [38] C.-L. Liu, W.-C. Chen, *Macromol. Chem. Phys.* 206 (2005) 2212–2222.
- [39] S. Dufresne, M. Bourgeaux, W.G. Skene, *Acta Cryst. E62* (2006) o5602–o5604.
- [40] W. Heinzelmann, H. Labhart, *Chem. Phys. Lett.* 4 (1969) 20–24.
- [41] S.K. Saha, S.K. Dogra, *J. Mol. Struct.* 470 (1998) 301–311.
- [42] L.J. Andrews, A. Derouede, H. Linschitz, *J. Phys. Chem.* 82 (1978) 2304–2309.
- [43] W.G. Skene, S. Dufresne, T. Trefz, M. Simard, *Acta Cryst. E62* (2006) o2382–o2384.
- [44] K.N. Campbell, A.H. Sommers, B.K. Campbell, *J. Am. Chem. Soc.* 66 (1944) 82–182.
- [45] N.I. Nijegorodov, W.S. Downey, *J. Phys. Chem.* 98 (1994) 5639–5643.
- [46] M. Montalti, A. Credi, L. Prodi, T. Gandolfi, *Handbook of Photochemistry*, Marcel Dekker, 2006.
- [47] J.R. Lakowicz, *Principles of Fluorescence Spectroscopy*, Springer, New York, 2006.
- [48] N.J. Turro, *Modern Molecular Photochemistry*, University Science Books, Sausalito, 1991.
- [49] A. Gilbert, J. Baggott, *Essentials of Molecular Photochemistry*, CRC Press, Boca Raton, 1991.
- [50] J.C. Scaiano, *CRC Handbook of Organic Photochemistry*, CRC Press, Boca Raton, 1989.
- [51] J.-M. Lehn, *Chem. Eur. J.* 12 (2006) 5910–5915.
- [52] J.-S. Wu, W.-M. Liu, X.-Q. Zhuang, F. Wang, P.-F. Wang, S.-L. Tao, X.-H. Zhang, S.-K. Wu, S.-T. Lee, *Org. Lett.* 9 (2007) 33–36.
- [53] G. Wettermark, J. Weinstein, J. Sousa, L. Dogliotti, *J. Phys. Chem.* 69 (1965) 1584–1587.
- [54] S.L. Murov, I. Carmichael, G.L. Hug, *Handbook of Photochemistry*, Marcel Dekker, Inc., New York, 1993.